HIGH-EFFICIENCY INDUSTRIAL-TYPE PERC SOLAR CELLS APPLYING ICP AlO_x AS REAR PASSIVATION LAYER

T. Dullweber[1], M. Siebert[1], B. Veith[1], C. Kranz[1], J. Schmidt[1,2], R. Brendel[1,2], B.F.P. Roos[3], T. Dippell[3], A. Schwabedissen[4], S. Peters[4]

[1]*Institute for Solar Energy Research Hamelin (ISFH), Am Ohrberg 1, D-31860 Emmerthal, Germany*
[2]*Department of Solar Energy, Institute of Solid-State Physics, Leibniz University of Hanover, Appelstrasse 2, D-30167 Hanover, Germany*
[3]*Singulus Technologies AG, Hanauer Landstrasse 103, 63796 Kahl am Main, Germany*
[4]*Q-Cells SE i.I., Sonnenallee 17 – 21, 06766 Bitterfeld-Wolfen, Germany*

ABSTRACT: Passivated emitter and rear cells (PERC) are considered to be the next generation of industrial-type screen-printed silicon solar cells. However, today there exist only few deposition methods for rear passivation layers which meet both, the high-throughput and low-cost requirements of the PV industry in combination with high-quality surface passivation properties. In this paper, we evaluate and optimize a novel deposition technique for AlO_x passivation layers applying an inductively coupled plasma (ICP) plasma-enhanced chemical vapour deposition (PECVD) process. The ICP AlO_x deposition process enables high deposition rates of up to 5 nm/s as well as excellent surface recombination velocities below 10 cm/s after firing. When applied to PERC solar cells the ICP AlO_x layer is capped with a PECVD SiN_y layer. We achieve independently confirmed conversion efficiencies of up to 20.1% for large-area (15.6x15.6 cm^2) PERC solar cells processed at ISFH with screen-printed metal contacts and ICP AlO_x/SiN_y rear side passivation on standard boron-doped Czochralski-grown silicon wafers. The internal quantum efficiency reveals an effective rear surface recombination velocity S_{rear} of (90 ± 30) cm/s and an internal rear reflectance Rb of (91 ± 1)% which demonstrates the excellent rear surface passivation of the ICP AlO_x/SiN_y layer stack. PERC solar cells processed in the Q-Cells Research Line achieve efficiencies up to 19.6% with ICP AlO_x/SiN_y rear passivation which is comparable to the reference process at Q-Cells.

Keywords: silicon solar cells, rear passivation, inductively coupled plasma, aluminium oxide, AlO_x, screen printing

1 Introduction

Passivated emitter and rear (PERC) solar cells are a very promising candidate for next-generation industrial-type screen-printed silicon solar cells. Excellent conversion efficiencies above 20.0% with record values up to 20.2% have been demonstrated by several companies and research institutes for large area, p-type PERC solar cells with screen-printed metal contacts [1,2,3,4]. Several production-type tools for the deposition of rear passivation layers are already available on the market [5,6] or under development [7,8]. In particular, rear passivation layers consisting of aluminium oxide (AlO_x) have attracted considerable attention due to their excellent surface passivation properties.

However, in addition to excellent electrical properties, it is also important that the AlO_x deposition process achieves high deposition rates and hence a high throughput which enables a low cost of ownership. Plasma-enhanced chemical vapour deposition (PECVD) processes applying an inductively coupled plasma (ICP) form a high-density plasma (HDP) with electron densities of around 10^{12} cm^{-3} [9] and hence allow high deposition rates of up to several nanometres per second [10]. ICP PECVD processes have been intensively investigated for the deposition of dielectric insulation and encapsulation layers consisting of SiO_x [11,12] or SiN_x [12,13,14]. The focus at that time was on applications in microelectronic manufacturing, e.g. as a final passivation layer or diffusion barrier. One important feature of the ICP-PECVD process is that the plasma density can be independently varied from the ion energy, which is typically lower than 30 eV. Hence, an independent optimization of the deposition rate versus the reduction of surface damage of the silicon wafer is possible. In recent years, Singulus Technologies commercialized the ICP-PECVD process for the deposition of SiN_x antireflection layers of silicon solar cells using their SINGULAR tool platform [10].

In this paper, we investigate the application of the ICP-PECVD process for the deposition of AlO_x layers. We deposit the ICP AlO_x layers using a laboratory-type tool at ISFH and investigate the surface passivation properties. We apply ICP AlO_x/SiN_y layer stacks as rear passivation to large-area PERC solar cells processed at ISFH as well as PERC cells processed at the Q-Cells Research Line. Finally, we present ISFH PERC cell results with an ICP AlO_x/SiN_y layer stack deposited in a SINGULAR production type tool developed by Singulus.

2. AlO_x deposition using an inductively coupled plasma (ICP)

The ICP AlO_x layers are deposited in a laboratory-type clustertool (Von Ardenne CS 400 P) at ISFH consisting of a load lock chamber, a transfer chamber and several PECVD deposition chambers including the ICP AlO_x chamber. Figure 1 displays a schematic drawing of the ICP AlO_x deposition chamber. A coil outside the vacuum chamber inductively excites the plasma using a high frequency generator with 13.56 MHz. As precursor gas we use trimethylaluminium (TMAl) and as a reactive gas oxygen (O2). The silicon wafer is transported on a carrier and electrically heated during the AlO_x deposition. Depending on the process parameters, we obtain high static deposition rates up to 5 nm/s while maintaining low ion energies below 30 eV. We vary the thickness of the resulting ICP AlO_x layers by adjusting the time of the deposition process. Afterwards, the ICP AlO_x passivation layers are covered with a µW-PECVD SiN_y capping layer (SiNA, Roth und Rau, or Singular, Singulus) in order to improve the firing stability and the optical reflectivity when applied to PERC solar cells.

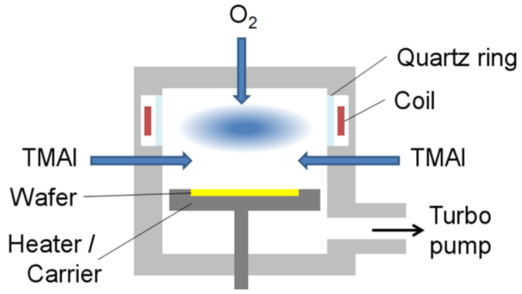

Figure 1: Schematic drawing of the laboratory-type ICP AlO_x deposition chamber. The plasma is inductively excited with a coil outside the vacuum chamber using TMAl and O_2 as process gases. The wafer is transported on a carrier and heated during deposition.

3 Surface passivation properties of ICP AlO_x layers

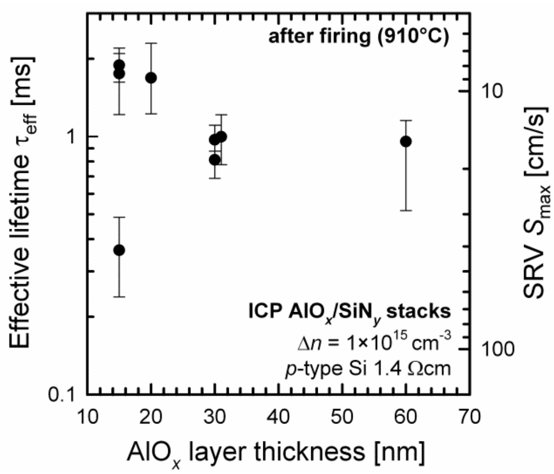

Figure 2: Effective carrier lifetime and corresponding surface recombination velocity measured on 1.4 Ωcm float zone (FZ) wafers in dependence of the ICP AlO_x layer thickness showing lifetimes of up to 2 ms and surface recombination velocities below 10 cm/s for ICP AlO_x layers covered with a µW-PECVD SiN_y layer (SiNA, Roth und Rau) after firing.

In order to determine the surface passivation properties, we deposit ICP AlO_x layers capped with a µW-PECVD SiN_y layer (SiNA, Roth und Rau) on both sides of p-type 1.4 Ωcm float zone (FZ) wafers and apply a typical firing process in a conveyor belt furnace with peak temperatures of 910°C. Afterwards we measure the minority charge carrier lifetime using the quasi-steady-state photoconductance (QSSPC) technique at a carrier density of $1x10^{15}$ cm^{-3}. From the measured lifetime τ_{eff} we deduce the maximum surface recombination velocity S_{max} attributing the whole recombination to the wafer surface by using the equation $S_{max} = W/2*\tau_{eff}$, where W is the wafer thickness. The QSSPC measurements reveal excellent effective lifetimes of up to 2 ms corresponding to surface recombination velocities (SRV) S_{max} below 10 cm/s for ICP AlO_x/PECVD SiN_y layer stacks after firing as displayed in figure 2. The error bars in figure 2 refer to the minimum and maximum values of the effective lifetimes measured on different positions on the same wafer revealing a good homogeneity of the surface passivation across the wafer. We see a moderate dependence of the SRV on the AlO_x layer thickness with the lowest value of 7,5 (±1,5) cm/s at 15 nm AlO_x thickness.

4 Application of ICP AlO_x/SiN_y layer stacks to high-efficiency screen-printed PERC cells processed at ISFH

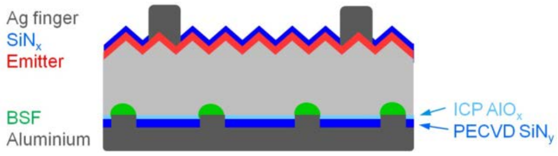

Figure 3: Schematic drawing of the PERC solar cells processed at ISFH with screen-printed front and rear contacts applying a ICP AlO_x/SiN_y rear passivation stack.

We apply the ICP AlO_x/SiN_y layer stacks as rear surface passivation to industrial type high-efficiency PERC solar cells with screen-printed metal front and rear contacts which are processed at ISFH. The process sequence of the PERC solar cells is very similar to the process sequence reported in detail in Ref. 15. Here we just highlight the most important process steps. We use industry-standard 156 x 156 mm^2, boron-doped Czochralski (Cz) silicon wafers with a resistivity of 2 – 3 Ωcm and a starting thickness of 200 µm. Before texturing and phosphorus diffusion, we deposit a dielectric protection layer on the rear side of the wafer leaving the rear side planar and non-diffused. We use a homogeneously doped phosphorus emitter with a sheet resistance of about 60 Ω/sq.

Afterwards, we deposit an AlO_x layer on the rear side with the ICP-PECVD deposition process as described above. We evaluate two different ICP AlO_x layer thicknesses of 20 nm and 30 nm and compare them to a 10 nm thick ALD Al_2O_3 layer as reference. We then deposit a µW-PECVD SiN_y (SINA, Roth und Rau) capping layer on top of the AlO_x passivation layer at the rear in order to improve both, the optical reflectivity as well as the surface passivation quality. Alternatively we deposit an ICP-PECVD SiN_y (Singular, Singulus) capping layer. Finally, we apply an ICP AlO_x/ ICP SiN_y layer stack with 30nm AlO_x thickness deposited completely in a SINGULAR production type tool developed recently by Singulus

The emitter is covered with a SiN_x anti-reflective coating. The dielectric layer stacks at the rear are locally ablated by laser contact opening (LCO) in order to form local line openings [16,17]. We choose line contacts instead of point contacts since line openings facilitate the formation of a deep and uniform local Al-BSF [18]. The Ag front contacts are deposited by a print-on-print (PoP) screen printing process resulting in a finger width of around 70 µm and a shadowing loss including bus bars of around 6.2% [19]. The Al rear contact is formed by full-area Al screen printing applying a commercially available Al paste designed for local rear contacts. A schematic drawing of the cross section of the resulting PERC solar cell is shown in figure 3 whereas figure 4 displays photographs of the front and rear side. The contact lines at the cell rear side as well as the rear passivation layer are clearly visible.

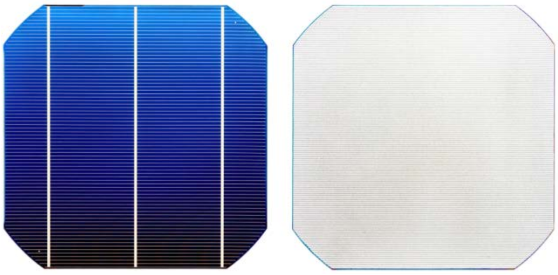

Figure 4: Photographs of the front and rear side of a PERC solar cell with 20.1% conversion efficiency. Whereas the front side is very similar to industry-standard screen-printed solar cells, the rear side shows the ICP AlO_x/SiN_y passivation layer and the local line contacts.

Table 1 summarizes the IV parameters of the best solar cells of each split group. The PERC solar cell with a 30 nm ICP AlO_x layer achieves an independently confirmed conversion efficiency of 20.1% which is one of the highest efficiencies reported so far for industrial-type PERC solar cells. The high V_{OC} of 655 mV and high J_{SC} of 39.0 mA/cm^2 indicate the excellent rear side passivation by the ICP AlO_x/ µW SiN_y stack. The PERC solar cells with the 20 nm ICP AlO_x layer exhibits similar IV parameters for both, µW (SiNA, Roth und Rau) and ICP SiN_y (Singular, Singulus) capping layers. The SINGULAR ICP AlO_x/ ICP SiN_y stack achieves efficiencies up to 19.8% and the reference PERC solar cell with ALD Al_2O_3/SiN_y rear passivation displays efficiencies up to 20.0%. Within statistical process variations and measurement errors, all rear passivation stacks show comparable results. Table 1 also includes the IV parameters of an industry standard screen-printed solar cell with full-area Al-BSF with a conversion efficiency of 18.7%. As can be seen by comparison, the strong efficiency improvement of the PERC solar cells compared to the full-area Al-BSF cell is mainly due to improved V_{OC} and J_{SC} values as a result of the improved electrical and optical properties of the rear side.

Table 1: IV parameters measured under standard testing conditions (STC) of 156 x 156 mm^2 p-type Cz PERC silicon solar cells processed at ISFH. The ICP AlO_x/SiN_y passivated cells achieve conversion efficiencies up to 20.1%.

AlO_x/SiN_y	AlO_x [nm]	η [%]	V_{oc} [mV]	J_{sc} [mA/cm^2]	FF [%]
ICP/µW	30	20.1*	655	39.0	78.8
ICP/µW	20	20.0*	657	39.1	77.8
ICP/ICP	20	19.9	650	39.2	78.3
SINGULAR	30	19.8	652	38.9	78.1
ALD/ICP	10	20.0	650	39.3	78.3
Al-BSF	-	18.7	638	37.1	79.1

*independently confirmed by FhG-ISE CalLab

Figure 5 shows the internal quantum efficiency (IQE) and the reflectance of the PERC solar cells of table 1. The rear passivation layer mainly impacts the reflectance and IQE in the wavelength range between 900 nm to 1200 nm. As can be seen in figure 5, in this wavelength range the PERC solar cells show almost identical IQE and reflectance values. We fit the experimental reflectance and IQE values in the infrared wavelength regime by assuming a bulk diffusion length of 1.3 mm and applying the software LASSIE [20] which combines the extended IQE evaluation by Basore [21] with the improved optical model developed by Brendel [22]. We obtain effective rear surface recombination velocities S_{rear} of 60 – 120 cm/s and internal rear reflectances R_b of 90 – 92% showing the excellent electrical and optical properties of the ICP AlO_x/SiN_y passivation stacks which are almost identical to the ALD Al_2O_3/SiN_y stack.

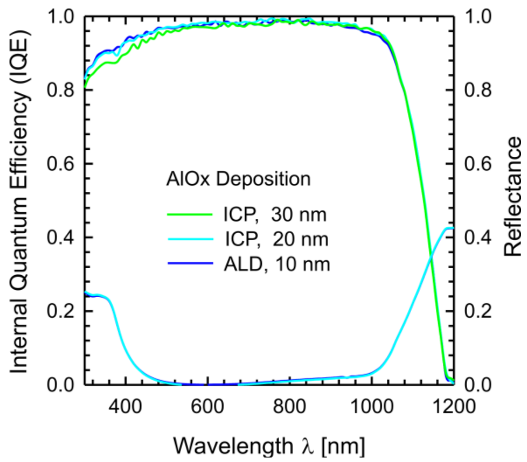

Figure 5: Internal quantum efficiency (IQE) and reflectance of the PERC solar cells of table 1. By analytical modeling we obtain S_{rear} values of 60 – 120 cm/s and an R_b of 90 – 92% showing the excellent electrical and optical parameters of the ICP AlO_x/SiN_y passivation stacks.

5 PERC solar cells with ICP AlO_x rear passivation processed at Q-Cells

In addition to the PERC cells processed at ISFH, we apply the ICP AlO_x process as rear passivation layer to PERC cells processed in the Q-Cells Research Line. We use 156 x 156 mm^2 p-type Cz as well as p-type multicrystalline silicon wafers. The solar cells are processed at Q-Cells up to the process step where the rear passivation layer is deposited. We then deposit the ICP AlO_x layer in the laboratory-type tool at ISFH on the rear side of the PERC cells. Back at Q-Cells, a SiN_y capping layer is deposited on top of the ICP AlO_x layer. The cell processing further includes full area Al screen printing on the rear as well as screen-printed Ag front contacts. The rear contacts are formed by laser fired contacts (LFC) [2,23]. In parallel, reference PERC cells are processed in the Q-Cells Research Line for all process steps including a reference rear surface passivation.

Table 2 summarizes the resulting solar cell parameters. Shown are the median values of 8 solar cells of the ICP AlO_x/SiN_y rear passivated cells as well as the median values of approx. 50 reference PERC cells. In general, the IV parameters of the ICP AlO_x/SiN_y passivated PERC cells are quite comparable to the reference process and demonstrate the high surface passivation quality of the ICP AlO_x/SiN_y layer stack. The best PERC cell achieves a conversion efficiency of 19.6% with ICP AlO_x/SiN_y rear passivation which compares to 19.8% as the best value for the reference cells.

Table 2: IV parameters measured under standard testing conditions (STC) of 156 x 156 mm^2 p-type Cz and multicrystalline PERC silicon solar cells processed at the Q-Cells Research Line. Shown are the median values of 8 solar cells of the ICP AlO_x/SiN_y rear passivated cells as well as the median values of approx. 50 reference PERC cells.

Rear Passivation	Wafer type	η [%]	V_{oc} [mV]	J_{sc} [mA/cm^2]	FF [%]
ICP AlOx	Cz	19.4	640	38.5	78.8
Reference	Cz	19.5	641	38.4	79.4
ICP AlOx	Multi	17.5	629	36.5	76.5
Reference	Multi	17.9	635	36.5	76.8

6 Conclusions

We have developed a novel deposition technique for AlO_x layers applying an inductively coupled plasma (ICP) PECVD deposition process which allows high deposition rates up to 5 nm/s. Experiments on test wafers demonstrate an excellent surface passivation quality of the resulting ICP AlO_x layers with surface recombination velocities after firing down to 7.5 cm/s when applying a SiN_y capping layer. Industrial-type PERC solar cells processed at ISFH applying an ICP AlO_x/SiN_y rear passivation stack demonstrate conversion efficiencies up to 20.1% which is one of the highest conversion efficiencies reported so far for industrial-type PERC solar cells. The IQE analysis reveals an excellent rear surface recombination velocity of (90±30) cm/s and a high internal optical reflectance of (91±1)%. In addition, PERC solar cells processed in the Q-Cells Research line with ICP AlO_x/SiN_y rear passivation achieve median conversion efficiencies of 19.4% on Cz wafers which is very comparable to the reference process with 19.5%. Accordingly, we demonstrate that the ICP-PECVD process is very well suited for the deposition of high quality AlO_x passivation layers. Singulus Technologies commercializes this novel passivation layer in the course of this year.

Acknowledgements

We thank our colleagues at ISFH for support in solar cell processing as well as Heraeus and Ferro for providing the screen printing pastes. We thank Tom Falcon from DEK for the fruitful collaboration on improving the front side screen printing process. This work was funded by the German Federal Ministry for the Environment, Nature Conservation and Nuclear Safety within the R&D projects HighScreen and ALBA II and by our industry partners Singulus Technologies, Rena, Schott Solar, Solar World, and Q-Cells.

References

[1] Schott Solar AG press release, August 2011, http://www.ffpress.net/Kunde/SOL/PM/12592330/

[2] P. Engelhart et al., Proceedings of the 26th European Photovoltaic Solar Energy Conference, Hamburg, Germany (2011) 821 - 826

[3] B. Veith, T. Dullweber, M. Siebert, C. Kranz, F. Werner, N.-P. Harder, J. Schmidt, B.F.P. Roos, T. Dippell, R. Brendel, Energy Procedia 27 (2012) 379-384

[4] K.A. Münzer, J. Schöne, M. Hein, A. Teppe, R.E. Schlosser, M. Hanke, J. Maier, K. Varner, S. Keller, and P. Fath, Proceedings of the 26th European Photovoltaic Solar Energy Conference, Hamburg, Germany (2011) 2292 – 2297

[5] H.-P. Sperlich, D. Decker, P. Saint-Cast, E. Erben and L. Peters, Proceedings of the 25th European Photovoltaic Solar Energy Conference, Valencia, Spain (2010) 1352 – 1357

[6] K.A. Münzer, M. Hein, J. Schöne, M. Hanke, A. Teppe, R.E. Schlosser, J. Maier, A.Yodyunyong, S. Krümberg, S. Keller, and P. Fath, Energy Procedia 27 (2012) 631 – 637

[7] P. Poodt et al., Adv. Mater. 22 (2010) 3564–3567

[8] P. G. Vermont, V. Kuznetsov, E. H. A. Granneman, Proceedings of the 26th European Photovoltaic Solar Energy Conference, Hamburg, Germany (2011) 1644 – 1647

[9] E. Kändler, G. Graßhoff, K. Drescher, Surface and Coatings Technology 74–75 (1) (1995) 539–545

[10] B. F. P. Roos, O. Hohn, T. Dippell, B. Cord, M. R. Huber, and P. Binkowska, Proceedings of the 24th European Photovoltaic Solar Energy Conference, Hamburg, Germany (2009) 1665 – 1668

[11] Y. Inoue, O. Takai, Plasma Sources Sci. Technol. 5 (1996) 339 – 343

[12] J. W. Lee, K. D. Mackenzie, D. Johnson, J. N. Sasserath, S. J. Pearton, and F. Renc, J. Electrochem. Soc. 147 (4) (2000) 1481-1486

[13] S.-S. Han, B.-H. Jun, K. No, and B.-S. Bae, J. Electrochem. Soc. 145 (2) (1998) 652 – 658

[14] J. Yota, J. Hander, and A. A. Saleh, J. Vac. Sci. Technol. A 18 (2) (2000) 372-376

[15] T. Dullweber, S. Gatz, H. Hannebauer, T. Falcon, R. Hesse, J. Schmidt, and R. Brendel, Prog. Photovolt (2011) DOI: 10.1002/pip.1198

[16] S. Gatz, H. Hannebauer, R. Hesse, F. Werner, A. Schmidt, T. Dullweber, J. Schmidt, K. Bothe, and R. Brendel, Phys. Status Solidi RRL 5 (2011) 147-149

[17] S. Gatz, J. Müller, T. Dullweber, and R. Brendel, Energy Procedia 27 (2012) 95-102

[18] J. Müller, K. Bothe, S. Gatz, H. Plagwitz, G. Schubert, and R. Brendel, IEEE Trans. Electron Devices 58 (10) (2011) 3239 - 3245

[19] H. Hannebauer, T. Falcon, R. Hesse, T. Dullweber, and R. Brendel, Proceedings of the 26th European Photovoltaic Solar Energy Conference, Hamburg, Germany (2011) 1607-1610.

[20] www.pv-tools.de

[21] Basore P A. Extended Spectral Analysis of Internal Quantum Efficiency, Proceedings of the 23rd IEEE Photovoltaic Specialists Conference, Louisville, USA, 1993; 147-152

[22] Brendel R. Thin-Film Crystalline Silicon Solar Cells. Wiley-VCH: Weinheim, 2003; 73

[23] E. Schneiderlöchner , R. Preu, R. Lüdemann, S. W. Glunz, Progress in Photovoltaics: Research and Applications 10, 29-34 (2002)